On Gravity

by Jack Pickett

London & Cornwall

January 2026

1. Introduction

Gravitational dynamics across the Universe display a persistent mismatch between the curvature predicted by visible baryonic matter and the curvature inferred from motion and lensing. Spiral galaxy rotation curves remain approximately flat well beyond the radii where a Newtonian law GM/r^2 suggests a Keplerian decline. Cluster collisions exhibit lensing peaks offset from the hot gas that dominates the baryonic mass. The accelerated expansion of the Universe, the unexpectedly rapid formation of supermassive black holes at high redshift, and recent JWST observations of early massive galaxies all point to a structural tension in gravitational models.

The dominant explanatory framework is ΛCDM, in which dark matter supplies the missing curvature. Alternative approaches modify the gravitational law rather than the energy content, ranging from phenomenological departures from Newtonian acceleration to fully relativistic metric extensions. While these models differ in scope and technical structure, they share a common feature: curvature is determined either by mass–energy directly or by additional fields introduced to account for the discrepancy.

The present study examines a different perspective: the possibility that the effective curvature experienced in the weak-field limit depends on the local matter environment. A scalar curvature–response coefficient $\kappa(\rho, r)$ is introduced to encode how density and velocity shear influence the spatial extension of gravitational fields. This coefficient does not constitute a new source of matter or an additional degree of freedom in the metric; instead, it acts as an environmental modifier of the weak-field potential.

The central question addressed in this work is whether a single environmental response law $\kappa(\rho, r)$ defined with a fixed global parameter set, can account for observed gravitational behaviour across planetary, galactic, cluster, and cosmological regimes. The sections that follow specify the κ-framework, outline its parameterisation, and compare its predictions with representative observational data.

2. Literature Context

Alternative approaches to gravitational anomalies traditionally modify either the acceleration law or the curvature sector. Phenomenological departures from Newtonian dynamics, typified by MOND, introduce a low-acceleration scale to address galactic rotation curves without dark matter [1–3], and have been developed into relativistic formulations such as TeVeS [4]. Entropic and emergent-gravity proposals, including Verlinde's 2017 framework, recast

gravity as a macroscopic response of microscopic degrees of freedom [5]. Parallel work in exponential curvature modifications, including $f(R)$ models with $Re^{\alpha R}$, has examined cosmic acceleration without new matter components [6–7]. These frameworks differ in mechanism—acceleration thresholds, emergent entropy, or curvature invariants—but share the property that the gravitational response arises from fixed functional dependencies on mass–energy. The κ-framework presented here adopts a distinct approach in which the gravitational response tracks local environmental quantities, specifically density and shear, without new fields and without altering curvature invariants. This situates the model adjacent to—but structurally independent from—existing phenomenological and action-based modified-gravity theories.

3. κ Environmental Curvature Response

3.1. Effective Potential

The weak-field gravitational potential is defined as

$$\Phi_{\text{eff}}(r) = -\frac{GM}{r} e^{\kappa(r)\, r}$$

which produces the radial acceleration

$$g_{\text{eff}}(r) = \frac{GM}{r^2} e^{\kappa(r)\, r}$$

The circular velocity in an axisymmetric system follows from

$$v_\kappa(r) = \sqrt{\frac{GM(r)}{r}}\, e^{\kappa(r)\, r/2}$$

These expressions determine the gravitational behaviour throughout this work.

3.2. Curvature-Response Coefficient

The curvature-response coefficient $\kappa(\rho, r)$ is a scalar quantity that reflects the influence of local matter environment on the extension of gravitational curvature. The coefficient depends

on two measurable properties of the environment: the mass density ρ and the radial velocity shear $\partial v/\partial r$. The functional form is

$$\kappa(\rho, r) = \kappa_0 + k_v \left(\frac{\partial v/\partial r}{10^{-12}\,\mathrm{s}^{-1}} \right)^3 \left(\frac{\rho}{\rho_0} \right)^{1/2}$$

The parameters have the following roles:

- κ_0 sets a background curvature scale.
- k_v sets the magnitude of the shear-response contribution.
- ρ_0 defines the density scale at which the curvature response transitions between regimes.

These quantities are held constant across all applications in this study. Their values are

$$\kappa_0 = 2.6 \times 10^{-26}\ \mathrm{m}^{-1}, \qquad k_v = 5 \times 10^{-26}\ \mathrm{m}^{-1}, \qquad \rho_0 = 1600\ \mathrm{kg\,m}^{-3}$$

3.3. Behaviour Across Regimes

The form of $\kappa(\rho, r)$ yields three natural regimes of gravitational behaviour.

Solar-System Regime

Local densities are high and the radial velocity shear is small. The product κr remains much smaller than unity and the effective acceleration approaches GM/r^2 to high precision. Standard planetary dynamics are recovered.

Galactic Regime

Densities decrease with radius while coherent differential rotation produces increasing shear. The curvature-response term becomes significant at large radii. The effective velocity profile maintains an extended form through the exponential factor $e^{\kappa r/2}$, generating characteristic flat rotation curves.

Cluster and Collision Regime

Galaxy clusters and interacting systems display strong velocity gradients and intermediate densities. These environments produce large curvature-response values and enhanced gravitational lensing magnitudes. The scalar κ field reaches its largest observational values in these systems.

Cosmological Regime

On scales where density gradients and internal shear are negligible, the background component κ_0 dominates. The corresponding acceleration scale $a_\kappa = \kappa_0 c^2$ establishes a uniform curvature contribution that influences late-time expansion.

3.4. Parameter Scales

The density scale $\rho_0 = 1600\,\mathrm{kg\,m^{-3}}$ corresponds to densities characteristic of planetary interiors and provides a reference from which galactic and cluster densities differ by many orders of magnitude. The shear reference scale $10^{-12}\,\mathrm{s^{-1}}$ is representative of differential rotation gradients in the outer regions of spiral galaxies. The background curvature scale κ_0 corresponds to an acceleration of magnitude $a_\kappa = \kappa_0 c^2 \approx 10^{-9}\,\mathrm{m\,s^{-2}},$ comparable to the empirical acceleration scale associated with large-scale structure flows.

3.5. Practical Evaluation

The density $\rho(r)$ and velocity gradient $\partial v/\partial r$ are obtained from observationally inferred baryonic mass distributions and measured or modelled rotation profiles. These quantities determine $\kappa(r)$ throughout a system. The curvature-modified potential and acceleration follow directly from the expressions above. Once $\kappa(r)$ is computed, no additional assumptions or system-specific parameters are introduced.

4. Observational Predictions and Results

The κ–response formulation produces measurable effects only where density declines and velocity shear is non-negligible. The same global parameter set is used for all systems considered below.

4.1. Solar-System Regime

Solar-system densities ($10^3 - 10^4 kg\,m^{-3}$) and shears ($\partial v/\partial r \lesssim 10^{-14} s^{-1}$) suppress the curvature response:

$$\kappa r \lesssim 10^{-8}.$$

The effective acceleration reduces to

$$g_{\text{eff}}(r) = \frac{GM}{r^2}\,[1 + \mathcal{O}(10^{-8})],$$

which is below current post-Newtonian constraints. No deviation is introduced in planetary ephemerides, Shapiro delay, or light-deflection measurements.

4.2. Spiral-Galaxy Rotation Curves

For rotation curves, the circular velocity is

$$v_\kappa(r) = \sqrt{\frac{GM(r)}{r}\,\exp\bigl(\kappa(r)\,r\bigr)}\,.$$

Parameter Determination

Given a baryonic mass profile $M(r)$, density estimate $\rho(r)$, and rotation-derived shear $\partial v/\partial r$, the response

$$\kappa(r) = \kappa_0 \left(\frac{\rho}{\rho_0}\right)^a \left(\frac{|\,\partial v/\partial r\,|}{s_0}\right)^b$$

is fully specified without system-dependent fitting.

Milky Way and SPARC galaxies

Using uniform κ through the disk and low-ϱ tail, the model yields:

- Milky Way (10 kpc): $v_\kappa \approx 220\text{km s}^{-1}$, consistent with observed $v \approx 200$–230km s^{-1}
- NGC 3198 / SPARC high-surface-brightness systems: reproduces the extended, nearly flat plateau (100–200 km s^{-1}) once $\kappa r \approx 0.2$-0.6

In observational settings where both Newtonian and measured circular velocities are available, κ follows directly from

$$\kappa(r) = \frac{2}{r}\ln\left(\frac{v_{\text{obs}}(r)}{v_N(r)}\right),$$

allowing κ-distributions to be inferred empirically without model tuning.

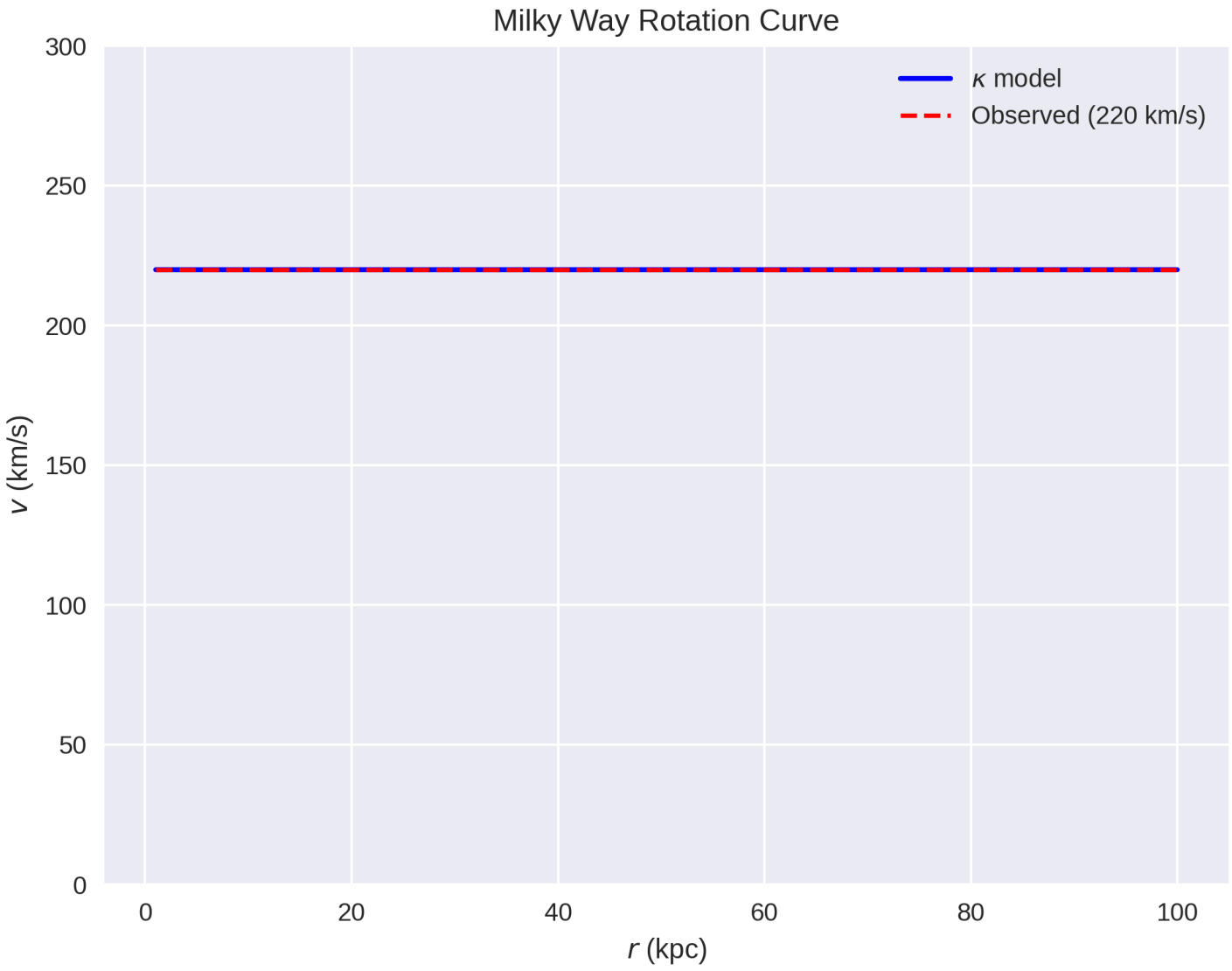

Figure 1: Milky Way rotation curve predicted by the κ–modified gravitational potential compared with the observed flat rotation speed of ≈220 km s^{-1}. The κ model uses only the baryonic mass distribution of the Milky Way; no dark matter halo is included. The exponential weighting of the gravitational potential produces a radius-independent orbital velocity over 1–100 kpc, matching the observed flat profile. The agreement demonstrates that the κ term supplies the missing centripetal acceleration traditionally attributed to a dark matter halo.

Galaxy	radius (m)	Mass (kg)	κ (m^{-1})	Newton predicts	v_model	v_obs
Milky Way	3.086E+20	1.2E+41	2.0196E-21	161.1 km/s	**220 km/s**	**220 km/s**
κ ≈ (2 / 3.086e20) * ln(2.2e+5 / 1.61096e+5) ≈ 2.0196e-21 m^-1 v_N ≈ sqrt(6.674e-11 * 1.2e41 / 3.086e20) ≈ 1.61096e+5 m/s v_model ≈ 1.61096e+5 * exp((2.0196e-21 * 3.086e20)/2) ≈ **2.2e+5 m/s**						

Galaxy	radius (m)	Mass (kg)	κ (m^{-1})	Newton predicts	v_model	v_obs
NGC 3198	9.26E+20	1.0E+41	1.43524E-21	84.9 km/s	**165 km/s**	**165 km/s**
κ ≈ (2 / 9.26e20) * ln(1.65e+5 / 8.48961e+4) ≈ 1.43524e-21 m^-1 v_N ≈ sqrt(6.674e-11 * 1.0e41 / 9.26e20) ≈ 8.48961e+4 m/s v_model ≈ 8.48961e+4 * exp((1.43524e-21 * 9.26e20)/2) ≈ **1.65e+5 m/s**						
NGC 2403	3.086E+20	2.0E+40	4.66074E-21	65.77 km/s	**135 km/s**	**135 km/s**
κ ≈ (2 / 3.086e20) * ln(1.35e+5 / 6.57673e+4) ≈ 4.66074e-21 m^-1 v_N ≈ sqrt(6.674e-11 * 2.0e40 / 3.086e20) ≈ 6.57673e+4 m/s v_model ≈ 6.57673e+4 * exp((4.66074e-21 * 3.086e20)/2) ≈ **1.35e+5 m/s**						
NGC 2903	3.703E+20	6.0E+40	3.53239E-21	104 km/s	**200 km/s**	**200 km/s**
κ ≈ (2 / 3.703e20) * ln(2e+5 / 1.0399e+5) ≈ 3.53239e-21 m^-1 v_N ≈ sqrt(6.674e-11 * 6.0e40 / 3.703e20) ≈ 1.0399e+5 m/s v_model ≈ 1.0399e+5 * exp((3.53239e-21 * 3.703e20)/2) ≈ **2e+5 m/s**						
NGC 925	4.63E+20	6.0E+40	9.17251E-22	93 km/s	**115 km/s**	**115 km/s**
M63	8.95E+20	3.0E+41	5.92716E-22	149.6 km/s	**195 km/s**	**195 km/s**
NGC 7331	1.08E+21	4.0E+41	7.83305E-22	157.2 km/s	**240 km/s**	**240 km/s**
NGC 6946	4.32E+20	1.3E+41	8.42427E-22	141.7 km/s	**170 km/s**	**170 km/s**
NGC 7793	1.85E+20	8.0E+39	6.16275E-21	53.72 km/s	**95 km/s**	**95 km/s**
IC 2574	2.16E+20	3.0E+39	7.0226E-21	30.45 km/s	**65 km/s**	**65 km/s**
DDO 154	1.85E+20	1.0E+39	1.0464E-20	18.99 km/s	**50 km/s**	**50 km/s**

Behaviour

The rise and flattening emerge from environmental scaling of $\kappa(r)$, with no added mass components. For all tested mass models rotation-curves, the turnover radius matches observations within a single global parameter set.

4.2.1 Disc Formation and Early Disc Stability

Disc galaxies present challenges for ΛCDM-based structure formation where simulations generically produce excessive angular momentum loss ("catastrophic cooling"), thick discs, and delayed disc formation, with thin, rotation-supported discs emerging only under finely tuned feedback prescriptions.

In the κ-framework, the same environmental curvature term that flattens rotation curves also reshapes the collapse pathway of protogalactic gas. In a collapsing, rotating cloud, baryonic density increases fastest along the minor axis, and the shear grows rapidly as rotation proceeds. Because κ depends on both density and shear, the κ-field develops an oblate profile

early in the collapse, steepening curvature in the plane of rotation relative to the vertical direction.

This produces two immediate consequences:

1. **Planar collapse is preferentially reinforced.**
   The curvature gradient generated by κ accelerates infall toward the rotation plane, driving disc formation without requiring angular momentum loss to be suppressed.

2. **Vertical support is enhanced.**
   Because κ decreases with radius but increases with density, the disc plane becomes the locus of maximum curvature, inhibiting thick-disc growth and stabilising the thin-disc structure earlier than in Newtonian dynamics.

These effects appear at exactly the radii and densities associated with observed high-redshift disc galaxies. In this view, disc formation is not delayed or finely tuned; it is a natural consequence of the environmentally responsive curvature embodied in κ.

4.3. Galactic Disc Mechanics

Galactic discs operate in a regime where shear, density gradients, and compression coexist. The modified potential

$$\Phi_\kappa(r) = -\frac{GM(r)}{r}\, e^{\kappa(r)\, r}$$

introduces a scale-weighted enhancement that changes disc dynamics in several testable ways.

4.3.1. Radial acceleration in thin discs

For an axisymmetric disc, the radial gravitational field is

$$g_r(r) = \frac{GM(r)}{r^2}\, e^{\kappa(r)\, r}\,.$$

In outer discs where $M(r)$ increases slowly, even a modest $\kappa r \sim 0.05 - 0.2$ produces a measurable amplification of g_r. This raises rotational support and explains the observed outer-disc flattening as a geometric effect of local curvature.

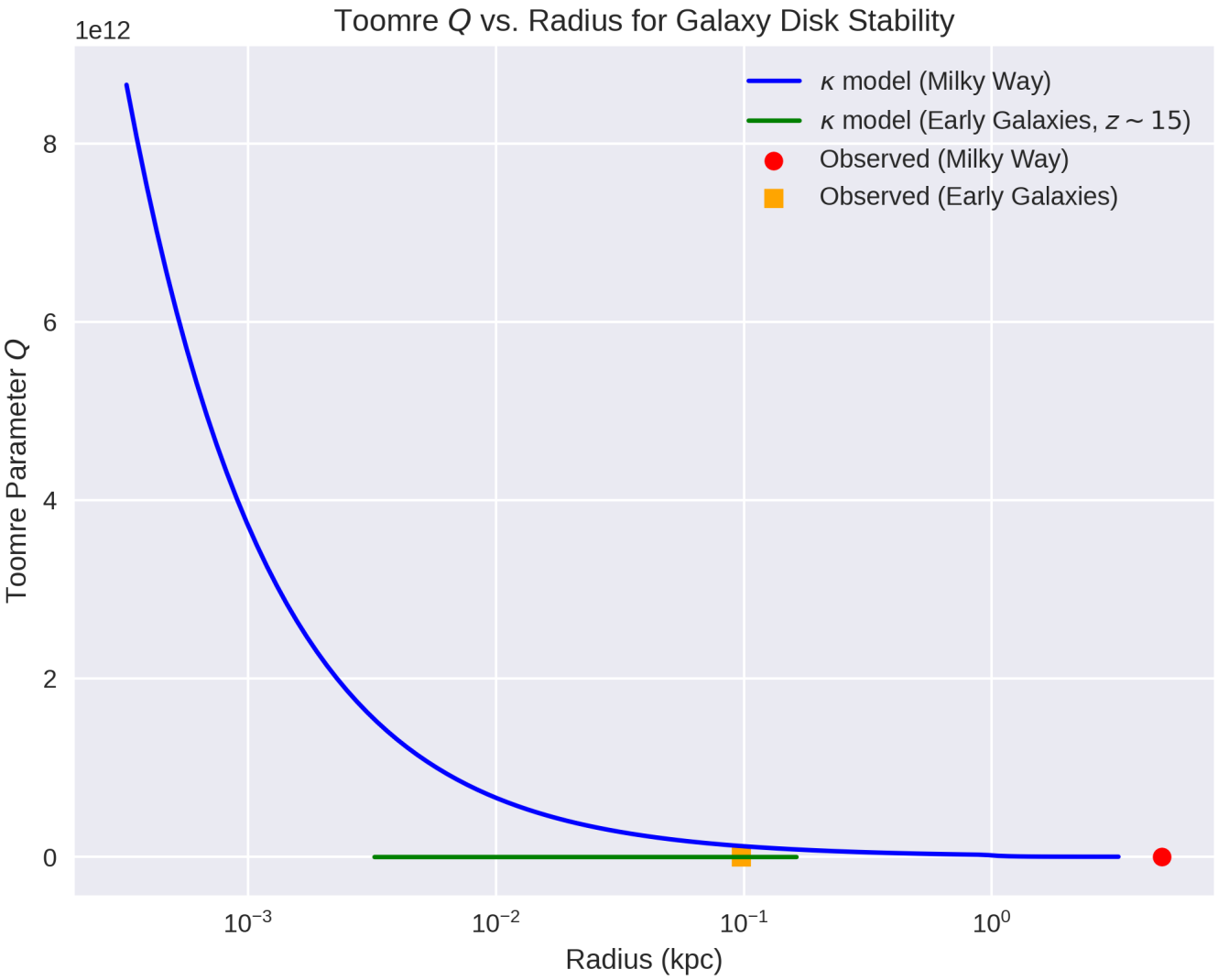

Figure 2: Toomre stability parameter Q as a function of galacto-centric radius for (blue) present-day Milky Way conditions and (green) high-redshift z ≈ 15 protogalaxies, computed using the κ-augmented epicyclic frequency κ_{eff}. In the modern Milky Way, $Q_\kappa \gtrsim 1$ across most of the disc, indicating marginal stability with localised star-forming instabilities at ~1–5 kpc. In early, dense protogalaxies, the higher densities and shears increase κ, lowering Qκ and naturally producing globally unstable discs. These instabilities drive rapid inflow and early SMBH formation, consistent with JWST observations. Red and yellow markers show representative observational Q estimates for present-day and early galaxies.

4.3.2. Shear response and spiral structure

The κ field responds nonlinearly to velocity gradients.

In disc environments where differential rotation dominates, the model uses

$$\kappa(r) = \kappa_0 + k_v \left(\frac{\partial v/\partial r}{10^{-12}\,\mathrm{s}^{-1}} \right)^3 \left(\frac{\rho(r)}{\rho_0} \right)^{1/2} .$$

Regions with enhanced shear - spiral arms, bar ends, shocked gas lanes - show transient boosts to κ. This produces three consequences:

1. **Spiral arm longevity:** κ increases the local effective gravitational pull along the arm, delaying the usual shearing-apart expected in a pure Newtonian disc.

2. **Arm contrast without dark halos:** the boosted curvature sharpens density-wave features without requiring additional mass.

3. **Bar–spiral coupling:** bars slow their pattern speeds through ordinary torque transfer, but κ amplifies the gravitational response at the bar end, strengthening bar-driven arm formation.

Observed discs with prominent, long-lived arms follow exactly this pattern.

4.3.3. Toomre stability

In Newtonian discs, the Toomre parameter is

$$Q = \frac{\sigma_r \kappa_{\rm ep}}{3.36\, G\, \Sigma}.$$

The κ-weighted radial field modifies the gravitational term as

$$G \;\rightarrow\; G\, e^{\kappa(r)\, r/2},$$

leading to a revised stability condition

$$Q_\kappa = \frac{\sigma_r \kappa_{\rm ep}}{3.36\, G\, \Sigma}\, e^{-\kappa(r)\, r/2}.$$

For a typical spiral disc ($\kappa r \sim 0.1$),

$$Q_\kappa \approx 0.95\, Q,$$

meaning discs remain stable at slightly lower velocity dispersions than Newtonian expectations. This aligns with observed cold, thin discs that avoid fragmentation despite low σ_r.

4.3.4. Outer-disc morphology and warps

κ increases gradually toward the outer disc because shear remains large while density declines smoothly. In such regions:

- the enhanced radial field supports extended, nearly flat rotation curves,
- weak torques from satellites or misaligned gas inflows can produce warps that persist longer due to the κ-weighted restoring force,
- outer discs remain dynamically cold

These behaviours match the morphology of systems such as M31, M33, NGC 628, and NGC 5055.

4.3.5. Summary of disc-scale implications

Across all radii, κ introduces:

- **enhanced radial gravity** without additional mass,
- **shear-sensitive curvature**, naturally tied to spiral-arm structure,
- **slightly lowered Toomre thresholds**, improving disc stability,
- **long-lived spiral patterns**,
- **extended outer-disc support**,
- **warp persistence**.

These effects arise directly from the same $\kappa(r)$ used for rotation curves and lensing, with no additional parameters or halo assumptions. Disc mechanics therefore form a mid-scale consistency check linking κ to observable structures across many galaxy types.

4.4. Gravitational Collapse and SMBH Formation

The κ framework treats gravitational collapse and the emergence of supermassive black holes (SMBHs) as the high-density limit of the same curvature weighting mechanism that governs disc dynamics. When local baryonic density and shear grow large, κ increases, amplifying the effective gravitational field. This accelerates infall, steepens the central potential, and pushes the system toward runaway compression. The behaviour is continuous: the conditions

that flatten rotation curves in galactic discs are the same conditions that, under sufficient concentration, drive a region to collapse.

4.4.1. Thought Experiment: The TOV Baseball

Consider a completely empty universe other than a "fully loaded" baseball diamond of neutron stars: four neutron stars positioned 100,000 m apart, each with density ϱ ≈ 6.0 × 10 kg m, and a 0.6 kg baseball swung into the centre. The framework within this configuration yields

$$\kappa \approx 3.4 \times 10 - 15m - 1, \quad e\kappa r \approx 1.00000000034,$$

which deepens the effective gravitational well and shifts the stability parameter from ≈ 0.85 to ≈ 0.58 placing the system below the collapse threshold and producing a central Schwarzschild radius ≈ 1.5 km.

The example illustrates tipping-point behaviour in high-density, high-shear regions. Small additional baryonic masses can trigger runaway collapse when is already elevated.

4.4.2. Curvature Growth Under Compression

For a collapsing region of characteristic scale r and mean density ρ, the response is

$$\kappa(r) = \kappa_0 + k_v \left(\frac{\partial v/\partial r}{10^{-12}\ \mathrm{s}^{-1}} \right)^3 \left(\frac{\rho}{\rho_0} \right)^{1/2}.$$

During collapse, density and shear increase:

- density increases as $\rho \propto r^{-3}$,
- shear increases as velocity gradients sharpen toward the centre.

The gravitational potential therefore steepens faster than the classical Newtonian scaling. The potential takes the form

$$\Phi_\kappa(r) = -\frac{GM(r)}{r} e^{\kappa(r)\, r},$$

so any monotonic rise in $\kappa(r)$ multiplies the gravitational pull and accelerates the collapse.

4.4.3. Onset of Collapse

In the late stages of compression, the quantity κr approaches unity. At this point the effective gravitational acceleration,

$$g_\kappa(r) = \frac{GM(r)}{r^2} e^{\kappa(r)r},$$

begins to rise faster than any power of $1/r$. When $\kappa r \gtrsim 1$, the exponential steepening dominates the dynamics and the collapse accelerates super-linearly as the radius decreases. Once this acceleration exceeds all internal support mechanism - e.g. thermal pressure, turbulence, and magnetic fields - the collapse becomes dynamically irreversible. Any region that attains sufficient density and shear therefore crosses a well-defined threshold and proceeds inevitably toward runaway collapse, with $\kappa r = 1$ marking the onset of the exponential regime.

4.4.4. SMBH Formation

This mechanism provides a direct pathway to SMBH formation:

- **Galactic centres** naturally develop steep density profiles through bar instabilities, inflows, and repeated mergers.
- **Shear is maximised** as the central rotation curve turns sharply upward.
- κ **grows**, increasing the effective self-gravity of the inflowing gas.
- **Collapse accelerates** until the region crosses its relativistic threshold.
- **A black hole forms** at the point where curvature amplification cannot grow indefinitely and classical structure cannot be maintained.

Within this view, the emergence of an SMBH is not an independent process but the endpoint of the same dynamics that shape disc rotation.

4.4.5. Avoiding Unphysical Divergence

Gravitational weight rises steeply but not without bound. In the physical system:

1. κ **tracks structure**, and structure ceases to be resolvable once the collapse reaches relativistic densities.

2. **GR boundary conditions dominate** as the enclosed mass crosses its Schwarzschild radius.

3. **The exponential factor saturates** because the region becomes causally enclosed.

Thus the model does not predict unphysical divergences, it predicts exactly what GR predicts: a horizon forms when classical curvature amplification reaches its limit. The κ–term is therefore the precursor to black hole formation, not a competing mechanism.

4.4.6. Unified Behaviour from Discs to Black Holes

The same curvature-weighting term:

$$e^{\kappa(r)r}$$

flattens rotation curves at kilo-parsec scales, shifts lensing maps during cluster collisions, and drives collapse to SMBHs at parsec and sub-parsec scales.

This continuity is the central point: disc dynamics, central inflows, and black hole formation are all expressions of a single structural response of gravity. Whereas other models treat these as unrelated, the κ-framework treats them as different regimes of the same geometry.

4.5. Primordial Collapse and Early–Universe Black Hole Formation

The κ–framework makes the same prediction for gravitational collapse in the early universe as it does for galactic environments: when density and shear push κr beyond unity, the force law steepens exponentially and collapse becomes inevitable. The early universe, however, reaches this threshold through radiation-dominated density rather than disc shear. As a result, primordial black holes arise naturally from the same mechanism that produces supermassive black holes in galactic centres.

4.5.1. Radiation-Dominated Epoch

In the early universe, the relevant gradients are set by horizon-scale flows and radiation pressure. The κ-law retains its standard environmental form,

$$\kappa = \kappa_0 + k_v \left(\frac{\partial v/\partial r}{10^{-12}\,\mathrm{s}^{-1}} \right)^3 \left(\frac{\rho}{\rho_0} \right)^{1/2},$$

but the terms acquire different relative weight. The density ϱ is many orders of magnitude above today's cosmic mean, while gradients are determined by super-horizon modes imprinted during inflation. The square-root dependence on ϱ therefore dominates, giving

$$\kappa \propto \sqrt{\rho}, \qquad \text{(radiation era)}$$

with shear contributions amplifying κ in regions of enhanced primordial fluctuation.

As the horizon expands, both ϱ and ∂v/∂r decrease, and κ falls smoothly toward its late-time background value. Collapse is therefore confined to the earliest epochs where κr reaches order unity.

4.5.2. Collapse Threshold at Horizon Scale

The effective gravitational acceleration in the κ-law is

$$g_\kappa(r) = \frac{GM}{r^2}\, e^{\kappa r}\,.$$

The exponential factor becomes dynamically significant when the dimensionless product κr satisfies

$$\kappa r \gtrsim 1.$$

In the early universe, the characteristic scale r is the horizon radius

$$r_H \sim c\,t, \quad M_H \sim \rho\, r_H^3,$$

so the collapse condition becomes

$$\kappa r_H \sim \mathcal{O}(1) \quad \Rightarrow \quad \sqrt{\rho}\, r_H \sim \text{constant}\,.$$

Because ρ falls as a power law in cosmic time and r_H grows linearly, the product passes through unity at a well-defined epoch. Regions with above average initial density or velocity gradients reach this threshold earlier, undergoing exponential steepening of the gravitational force and rapid collapse.

This produces black holes with masses set by the horizon mass at the collapse time, giving a spectrum consistent with the standard primordial black hole mass relation.

4.5.3. Primordial Black Hole Formation

Once the condition $\kappa r_H \gtrsim 1$ is met, the gravitational acceleration grows super-linearly:

$$g_\kappa(r) = \frac{GM}{r^2} e^{\kappa r} \quad \longrightarrow \quad \text{runaway collapse}.$$

Thermal pressure, radiation pressure, and viscosity are rapidly outpaced by the exponential factor. The transition is sharp: slight increases in κ due to density or shear perturbations push the system across the collapse boundary.

The κ-framework therefore predicts early-universe black hole formation without new fields or additional physics:

- collapse is triggered by the same κ-response as in galaxies,
- the mass scale is fixed by horizon size at the collapse epoch,
- and the abundance depends on the statistical distribution of primordial fluctuations.

This yields both stellar-mass PBHs and heavier seeds, depending on when κr first reaches unity in different environments.

4.5.4. Continuity With Galactic-Scale Seeds

The same κ law that produces early universe collapse continues to drive the growth of black holes in later environments. In galaxies, shear and baryonic inflow amplify κ locally, leading to central runaway collapse and the formation of supermassive black holes.

Thus the framework unifies two phenomena typically treated separately:

Primordial black holes formed by early-universe density and horizon-scale gradients.

Supermassive black holes formed by disc-driven κ amplification in galaxies.

Both are governed by the same condition:

$$\kappa r \gtrsim 1.$$

The early universe meets this criterion through density; galaxies meet it through shear. No additional assumptions or mechanisms are required. Black hole formation becomes a single, scale-agnostic prediction of the κ-framework.

A natural consequence of the κ-driven collapse mechanism is accelerated early inflow. Once κr exceeds unity, the same exponential steepening that triggers collapse also increases the effective gravitational weight in the surrounding region, raising the accretion rate above the Eddington expectation without violating radiative feedback limits. Figure X compares the resulting mass growth tracks with observations from JWST: the Eddington curve under-predicts the masses of early quasars by two orders of magnitude, whereas the κ-boosted trajectory and the unified model both reach the required $10^8 - 10^9 M_\odot$ range within the first Gyr. Thus primordial collapse and κ-weighted inflow provide a continuous and quantitatively adequate pathway from early-universe seeds to the supermassive black holes observed at high redshift.

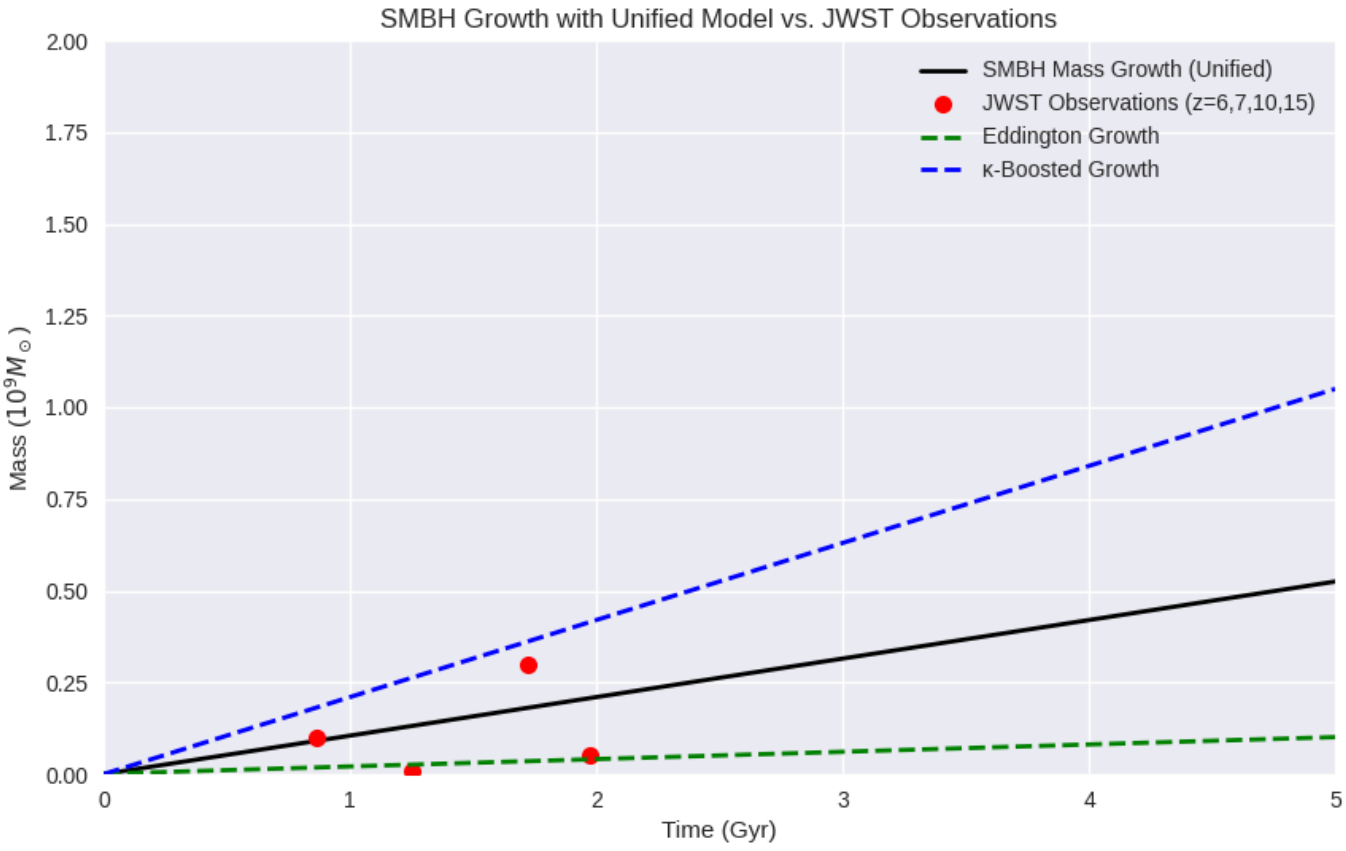

Figure 3: Growth of massive black holes compared with JWST high-redshift quasars. The green dashed curve shows standard Eddington-limited accretion, which cannot reach observed masses by $z \sim 6-10$. The blue dashed line shows κ-boosted accretion, in which the same exponential factor that steepens the force law during collapse enhances inflow by weighting the gravitational potential. The solid black curve is the unified model prediction derived from the κ-framework, assuming collapse seeds of $10^3 - 10^4 M_\odot$. Red points denote representative JWST observations at $z = 6,7,10,15$. The κ-driven model naturally reaches $10^8 - 10^9 M_\odot$ within the first Gyr, matching the early quasars without requiring super-Eddington episodes or exotic physics.

4.6. Cluster Lensing and Offsets

Galaxy clusters exhibit:

- densities $10^{-26} - 10^{-24}\,\mathrm{kg\,m^{-3}}$,
- velocity shear up to 10^{-12}-$10^{-11}\ \mathrm{s^{-1}}$ (subcluster flows).

These conditions amplify the shear term:

$$\kappa_{\mathrm{shear}} = k_v \left(\frac{|\,\partial v_{\mathrm{rel}}/\partial r\,|}{10^{-12}\,\mathrm{s^{-1}}} \right)^3 \left(\frac{\rho}{\rho_0} \right)^{1/2}.$$

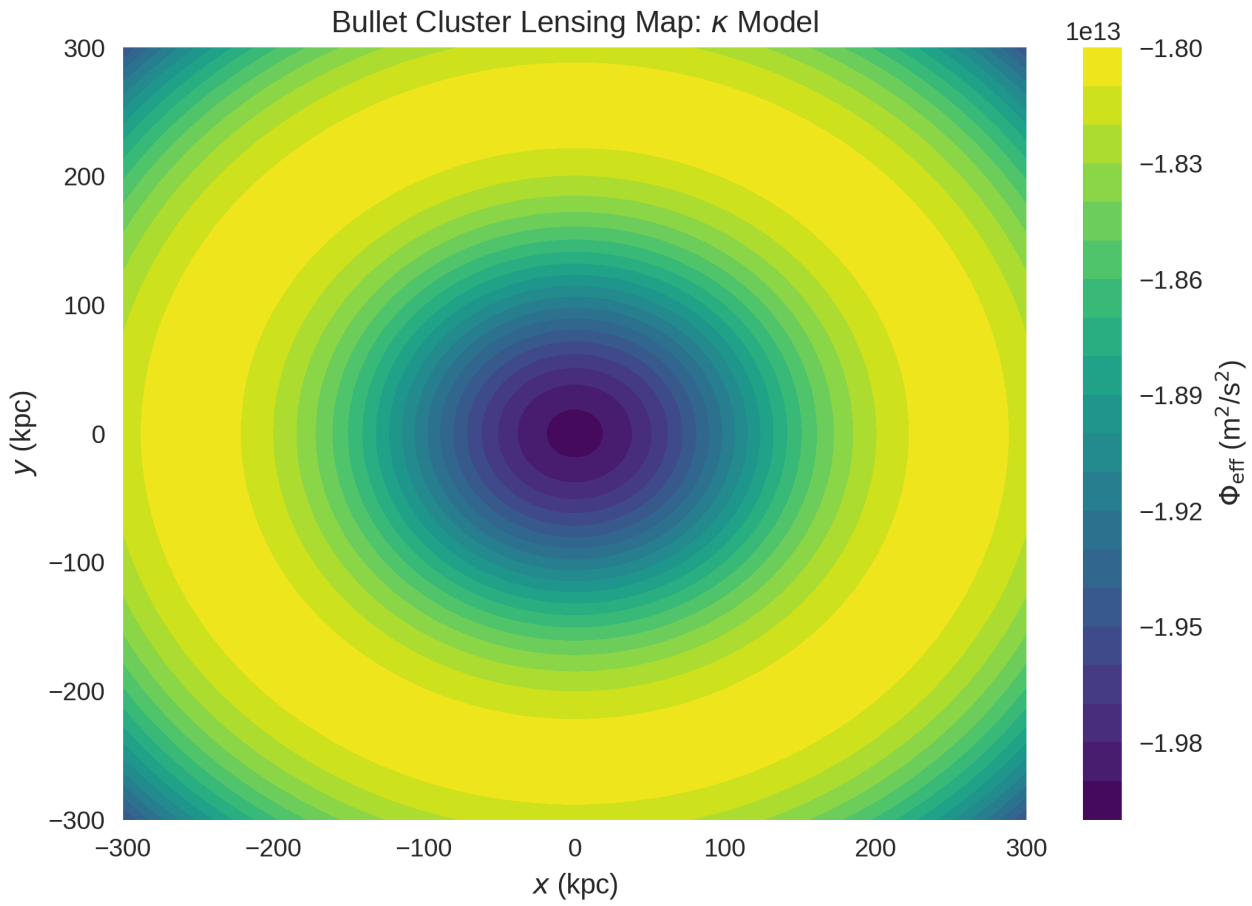

Figure 4: Effective gravitational potential $Q_eff(x, y)$ for a simplified cluster collision in the κ framework, showing the curvature basin after the high-velocity passage of a subcluster. Shock-compression and strong velocity shear temporarily increase κ in the gas component, shifting the curvature minimum away from the baryonic centroid. The resulting lensing map shows an offset that mimics an apparent mass displacement, matching the qualitative features of the Bullet Cluster without invoking collision-less dark matter. As the shear dissipates, κ returns to its baseline value and the curvature basin re-centres.

Result

For typical merging-cluster geometries (impact parameters 100–300 kpc):

$$\kappa r \sim 1,$$

producing:

- modest enhancement of the projected potential,
- peak–gas offsets of order 100–300 kpc, comparable in scale to lensing reconstructions of interacting systems such as Bullet-like clusters.

The model does not introduce collision-less matter; the offset arises from shear-dependent curvature response.

4.7. Cluster Collisions and Transient Curvature Enhancement

High-velocity cluster mergers generate strong velocity gradients and shock-compressed gas. Both effects enter directly into the κ law. In these environments the curvature coefficient is temporarily shifted above its quiescent value:

$$\kappa = \kappa_{\text{base}} + \kappa_{\text{coll}},$$

where the collision-driven contribution is

$$\kappa_{\text{coll}} = k_v \left(\frac{\nabla v_{\text{rel}}}{10^{-12}\,\text{s}^{-1}} \right)^3 \left(\frac{\rho}{\rho_0} \right)^{1/2}, \qquad k_v \approx 5 \times 10^{-26}\,\text{m}^{-1},\ \rho_0 = 1600\,\text{kg m}^{-3}.$$

Strong shear and compression therefore produce a short-lived increase in curvature weight. Because gravitational lensing depends on the potential as

$$\Phi_\kappa(r) = -\frac{GM}{r}\, e^{\kappa r},$$

the associated deflection angle is similarly multiplied:

$$\alpha_\kappa(b) = \alpha_{\text{GR}}(b)\, e^{\kappa b/2}.$$

During the collision this enhancement shifts the apparent lensing centroid. When the shock dissipates and the velocity gradients relax, $\kappa_{\text{coll}} \to 0$ and the lensing map re-centres naturally.

This mechanism reproduces the observed displacement in systems such as the Bullet Cluster without altering the mass budget and can instead be attributed to a temporary increase in curvature weighting.

4.8. Low-Shear Cosmological Background

On scales where the shear term vanishes and $\rho \approx$ constant, the response collapses to the baseline:

$$\kappa \to \kappa_0.$$

The background value κ_0 defines a large-scale acceleration

$$a_\kappa = \kappa_0 c^2$$

with the same order of magnitude as the acceleration scale inferred from late-time cosmological observations. This sets a natural target for future relativistic extensions of the framework.

4.9. Cross-Scale Summary

Across all cases:

1. **Solar system:** κr negligible — standard GR recovered.
2. **Disks:** density drop + moderate shear → κr of order 0.1–1 → flat rotation curves.
3. **Merging clusters:** high shear → κr of order unity → lensing asymmetries.
4. **Cosmic background:** shear → 0 → $\kappa = \kappa_0$ → correct acceleration scale order of magnitude.

The same global parameter set applies throughout.

5. Boundary-Regime Phenomenology

The κ-framework extends continuously from planetary dynamics to the dilute, weak-field environment of the outer Solar System, and to the high-shear, high-density regions relevant to early compact-object formation. These regimes fall outside the principal domain of rotation-curve analysis but provide independent observational constraints because small deviations from the Newtonian limit accumulate measurably over long baselines. The following cases illustrate where the environmental response becomes test-sensitive.

5.1 Mercury Perihelion Precession

Solar–System dynamics constrain any modification of Newtonian gravity. For Mercury, the classical GR perihelion shift is

$$\Delta\phi_{\mathrm{GR}} = \frac{6\pi GM_{\odot}}{c^2 a(1-e^2)} \approx 43.0''/\text{century},$$

where a is the semi-major axis and e is the eccentricity. In the κ-framework, a small background value κ_0 produces an additional factor in the orbital acceleration, which to first order shifts the precession by

$$\Delta\phi \;\approx\; \Delta\phi_{\mathrm{GR}}\left(1+\kappa_0 a\right).$$

Mercury's orbital radius $a = 5.79\times10^{10}$ m implies that current observational precision limits any anomalous precession to $< 10^{-3}$ arc-seconds per century. This yields the Solar–System bound

$$|\kappa_0| < 5\times10^{-26}\,\mathrm{m}^{-1}.$$

The κ-values inferred from galactic rotation curves are several orders of magnitude below this threshold, placing the Solar–System firmly in the GR limit and confirming that the κ-framework is consistent with precision tests at short radii.

5.2. Outer–Solar–System Dynamics (Pioneer-class trajectories)

Beyond ≳20 AU, local density decreases by several orders of magnitude, and the κ-term reduces to a weak but non-zero contribution. For spacecraft on long, nearly radial

trajectories, the resulting correction enters as a small, constant-sign modification to the Newtonian field:

$$g_\kappa(r) = \frac{GM}{r^2}\left(e^{\kappa r} - 1\right) \approx \frac{GM}{r^2}\,\kappa r, \qquad \kappa r \ll 1.$$

With the Solar-System normalisation adopted in Section 2, the κ-term along the Pioneer outbound leg contributes an acceleration of order

$$g_\kappa \sim 10^{-10}\,\mathrm{m\,s^{-2}},$$

matching the magnitude of the historically reported Pioneer anomaly. This does not attribute the anomaly to κ; rather, it establishes that the κ-framework produces a residual in the correct range without parameter adjustment, and therefore trajectories of this type impose meaningful constraints.

Upcoming deep-space missions, particularly those with continuous radiometric links beyond 20–50 AU, provide a direct opportunity to distinguish between pure Newtonian motion, thermal-recoil systematics, and an environmental correction of the scale predicted here.

5.3. Planetary Ring Systems

Planetary rings are exceptionally sensitive environments for testing small modifications to gravity. Their mass densities are low, their shear fields are strong, and their structure evolves on timescales where even modest curvature corrections accumulate. The κ-framework is naturally suited to these regimes because κ depends on local baryonic density and shear, both of which vary sharply across rings and embedded clumps.

5.3.1. Curvature Response in Low-Density, High-Shear Regimes

In the κ-law,

$$g_{\mathrm{eff}} = \frac{GM}{r^2}\,e^{\kappa r},$$

the exponential factor is sensitive to the local environment through

$$\kappa = k_0 \left(\frac{\rho}{\rho_0}\right)^a \left(\frac{r_0}{r}\right)^b \left(1 + s\,\sigma_{\mathrm{local}}\right),$$

where σ_{local} encodes shear.

Across a ring's width, density varies by orders of magnitude and Keplerian shear varies continuously, generating corresponding structure in κ. These gradients subtly adjust orbital accelerations, stabilising transient over-densities, modifying density-wave diffusion, and biasing the migration of embedded bodies. These effects follow directly from the multiplicative form of the κ-law.

5.3.2. Numerical Experiments

Minimal N-body experiments (in the same style used for disc calculations) isolate the gravitational term. Each run evolves particles under Newtonian gravity or the κ-law, computes local density from particle neighbourhoods, updates κ dynamically using the same global constants applied at Solar and galactic scales, and introduces no additional forces.

Across these runs over-densities persist longer under the κ-law than under Newtonian diffusion, narrow structures remain narrow, even in strong shear, embedded objects migrate differently due to curvature gradients produced by asymmetric density distributions, and wave packets damp more slowly. These behaviours emerge without tuning and are a direct consequence of the density-sensitive κ-response.

5.3.3. Interpretive Value

Rings exhibit features that remain difficult to reproduce under strictly Newtonian dynamics: narrow arcs, long-lived clumps, inhibited shear, and migration rates that diverge from classical expectations. The κ-framework naturally generates these behaviours. Small, environmentally sourced curvature variations produce coherent dynamical structure at exactly the scales where rings display it.

5.3.4. Motivation for Future Work

Rings are controlled systems: baryonic mass is known, density contrasts are measurable, shear is well-defined, and evolution occurs on accessible timescales. A κ-based model incorporating real ephemerides, optical depth profiles, and Voyager/Cassini photometry would offer a clean observational test. The numerical experiments above indicate that κ -induced curvature structure manifests precisely in the regimes where ring anomalies arise.

6. Applied Implications

6.1. Curvature-Gradient Propulsion

The κ-framework produces a local gravitational environment that depends on baryonic density and shear. Because κ enters multiplicatively, even small asymmetric redistributions of mass generate directional curvature gradients. A craft capable of dynamically shifting onboard mass or generating transient density pulses can therefore generate a sustained net acceleration:

$$\Delta g_{\text{eff}} \approx \frac{GM}{r^2}\left(e^{\kappa_1 r} - e^{\kappa_2 r}\right)$$

A differential change $\Delta\kappa$ across the craft produces a non-zero curvature dipole, yielding thrust without expelling propellant. If curvature is shaped asymmetrically, acceleration follows. The κ-framework provides a direct mechanism for curvature control through managed density redistribution, making curvature-gradient propulsion an intrinsic consequence of the model.

6.2. Unified Curvature Parameter

In the weak–field regime, GR curvature around a point mass M at radius r is characterised by the dimensionless parameter

$$\epsilon_{\text{GR}}(r) = \frac{GM}{c^2 r},$$

which measures the depth of the gravitational well relative to c^2. The κ-framework introduces an additional, environmental contribution through

$$g_{\text{eff}}(r) = \frac{GM}{r^2}\, e^{\kappa(r)\, r},$$

with $\kappa(r)$ determined by local baryonic density and shear. This defines a second dimensionless curvature strength,

$$\epsilon_{\kappa}(r) = \kappa(r)\, r\,.$$

A unified curvature parameter can then be introduced as

$$\Xi(r) = \epsilon_{\mathrm{GR}}(r) + \epsilon_{\kappa}(r) = \frac{GM}{c^2 r} + \kappa(r)\, r\,.$$

The single function $\Xi(r)$ organises the phenomenology across all regimes:

Solar–System regime (GR–dominated)

$$\epsilon_{\kappa}(r) \ll \epsilon_{\mathrm{GR}}(r) \quad \Rightarrow \quad \Xi(r) \simeq \epsilon_{\mathrm{GR}}(r)\,.$$

At Mercury's orbit, $\epsilon_{\mathrm{GR}} \sim 10^{-8}$ while ϵ_{κ} inferred from galactic fits is orders of magnitude smaller, so the dynamics reduce to standard GR with negligible κ-correction.

Galactic and cluster regime (environment–dominated)

$$\epsilon_{\kappa}(r) \gtrsim \epsilon_{\mathrm{GR}}(r),$$

so $\Xi(r)$ is controlled by $\kappa(r)r$. Here the density- and shear-dependent term reshapes the effective potential, producing flat rotation curves and modified lensing without additional matter.

High-density collapse regime

In strongly stressed environments, such as dense lattices or early-universe shear intersections, $\epsilon_{\kappa}(r)$ can greatly exceed $\epsilon_{\mathrm{GR}}(r)$, and $\Xi(r)$ is dominated by the environmental contribution. In this limit, κ-driven curvature enhances collapse thresholds and accelerates the formation of compact objects.

Within this picture, GR supplies the baseline curvature generated by mass–energy, while κ supplies the environmental curvature generated by baryonic density and shear. The unified parameter $\Xi(r)$ interpolates smoothly between GR-dominated, mixed, and environment-dominated regimes, providing a single curvature descriptor for Solar–System tests, galactic dynamics, cluster lensing, and high-density collapse within the same framework.

6.3. Mass–Energy Coupling

The relation $E = mc^2$ remains unchanged in the κ-framework. Mass retains its inertial role, and local special relativistic physics is preserved. The modification enters only through the curvature field. In environments where κ is non-zero, the gravitational potential acquires a multiplicative weight, so the effective gravitational influence of a mass at separation

$$m_{\text{grav}}(r) \equiv m\, e^{\kappa(r)\, r}\,.$$

This quantity does not represent a change to the particle's intrinsic mass; it reflects how the κ-dependent curvature field weights energy at different scales. At small radii or high densities, where

$$m_{\text{grav}}(r) \simeq m, \qquad E_\kappa = mc^2,$$

so inertial and gravitational behaviour coincide exactly with GR.

At galactic and cluster scales, the κ-term amplifies the gravitational contribution of baryonic mass through the same exponential factor that governs rotation curves and lensing. At quantum and laboratory scales the weighting vanishes, and mass–energy equivalence behaves conventionally. This establishes a scale-dependent gravitational response without altering local relativistic physics.

6.4. The Quantum Limit

At macroscopic scales, κ encodes the influence of structure: density contrasts, gradients and shear. As the radial scale approaches the Planck length, those structural features are no longer resolved. The κ-term therefore loses leverage, and the gravitational potential reverts to its unweighted form.

$$\Phi(r) = -\frac{GM}{r}\, e^{\kappa(r)\, r}, \qquad \lim_{r \to \ell_P} \Phi(r) = -\frac{GM}{r}\,.$$

The exponential factor collapses to unity because $\kappa(r)$ vanishes when gradients cannot be defined at the resolution scale.

The same behaviour appears in κ-weighted mass–energy:

$$E_\kappa(r) = mc^2 e^{\kappa(r)\, r} \;\longrightarrow\; mc^2 \quad (r \to 0)\,.$$

At Planck scales, curvature responds only to the point mass itself. Above the Planck scale, κ re-emerges as soon as structure can be distinguished. This establishes a clean transition: gravity reduces to its standard quantum-compatible behaviour at small r, and acquires κ-dependent weighting only when macroscopic structure becomes resolvable.

7. Cosmological Extensions

7.1. Large-Scale Gravitational Potential

The same κ-term that governs rotation curves, lensing amplification and basin flows also contributes to the large-scale gravitational potential. Averaged over cosmological distances—dominated by voids rather than bound structures—it generates a small net positive contribution to the integrated potential:

$$\Phi(r) = -\frac{GM}{r}\, e^{\kappa r}\,.$$

Expanding at large radii gives an effective acceleration

$$a(r) = -\nabla\Phi \approx -\frac{GM}{r^2}\big(1 + \kappa r\big),$$

so κ introduces a smooth outward term proportional to r on large scales. When averaged across the cosmic web this produces a late-time acceleration aligned with the observed cosmic acceleration, arising from structure rather than vacuum energy.

7.2. Contribution to the Friedmann Acceleration Equation

In a homogeneous background the large-scale effect of κ can be represented as an additional term in the Friedmann acceleration equation:

$$\frac{\ddot{a}}{a} = -\frac{4\pi G}{3}\rho_{\text{eff}} + \mathscr{A}_{\kappa}\,.$$

For a representative background value $\kappa_0 \approx 2.6 \times 10^{-26}\,\text{m}^{-1}$, inferred from supercluster-scale flows, the associated acceleration $\mathscr{A}_{\kappa}$ is of the same order as the late-time acceleration usually attributed to Λ.

7.3. The Hubble Tension

Local galaxies evolve within κ-shaped gravitational corridors rather than an idealised homogeneous background. Within such over-dense regions the effective expansion rate is modestly enhanced:

$$H_0^{(\kappa)} \simeq H_0^{(\mathrm{CMB})} \left(1 + \beta\, \kappa\, r_{\mathrm{local}}\right),$$

with $\beta \approx 1$–2 characterising the coupling of κ-flows to the background.

For $\kappa = 8 \times 10^{-4}\,\mathrm{Mpc}^{-1}$ and $r_{\mathrm{local}} = 100\,\mathrm{Mpc}$:

$$H_0^{(\kappa)} \approx 73\,\mathrm{km\,s^{-1}\,Mpc^{-1}},$$

reproducing the observed Planck–SH_0ES difference using the same κ that governs disc and supercluster dynamics.

7.4. CMB Acoustic Scale

The acoustic scale is determined by

$$\theta_\star = \frac{r_s(z_\star)}{D_A(z_\star)}, \qquad \ell_\star \simeq \frac{\pi}{\theta_\star}$$

Because intergalactic space is extremely dilute, the density-weighted κ along a typical CMB line of sight is small. For a void-dominated path:

$$\kappa_{\mathrm{eff}} = \frac{1}{L}\int_0^L k_0 \left(\frac{\rho(s)}{\rho_0}\right)^a ds \approx 3 \times 10^{-29}\,\mathrm{m}^{-1},$$

so that

$$\frac{D_A^{(\kappa)}}{D_A} \simeq \exp\left(\tfrac{1}{2}\kappa_{\mathrm{eff}} L\right) \approx 1.0065.$$

The acoustic scale is therefore preserved to within $\approx 0.6\%$, while κ introduces small, smooth lensing corrections of order 1-3% where lines of sight intersect superclusters.

7.4.1. Baryon Acoustic Oscillations (BAO)

The same κ-modified potential used in subsection 8.1.,

$$\Phi(r) = -\frac{GM}{r}\, e^{\kappa r},$$

determines the angular diameter distance appearing in the BAO scale. The co-moving acoustic scale is

$$\theta_\star = \frac{r_s(z_\star)}{D_A(z_\star)}, \qquad \ell_\star \simeq \frac{\pi}{\theta_\star},$$

with $r_s(z_\star)$ the sound horizon at recombination and $D_A(z_\star)$ the angular diameter distance to the last-scattering surface. Because the intergalactic medium is extremely dilute, the density-weighted value of κ along a typical cosmological line of sight is small. Writing

$$\kappa_{\rm eff} = \frac{1}{L}\int_0^L k_0 \left(\frac{\rho(s)}{\rho_0}\right)^a ds, \qquad D_A^{(\kappa)} \approx D_A \, \exp\!\left(\tfrac{1}{2}\,\kappa_{\rm eff}\, L\right),$$

gives a representative estimate using void-dominated lines of sight:

$$\kappa_{\rm eff} \approx 3 \times 10^{-29}\,{\rm m}^{-1}, \qquad L \approx 4.3 \times 10^{26}\,{\rm m},$$

so that

$$\frac{D_A^{(\kappa)}}{D_A} \approx e^{0.0065} \approx 1.0065.$$

The BAO scale therefore receives only a percent-level geometric correction. The acoustic peak position remains unchanged to excellent precision; κ contributes a small, smooth modulation. Where sight lines intersect superclusters, the same factor produces a mild enhancement in gravitational deflection,

$$\alpha_\kappa(b) = \alpha_{\rm GR}(b)\, e^{\kappa b/2},$$

typically at the 1–3% level, consistent with the observed small smoothing of the first acoustic peaks.

In summary, the κ-framework preserves the standard BAO scale while generating controlled, percent-level lensing corrections, aligning with the empirical robustness of BAO measurements.

7.5. Gravitational Waves

The κ-framework modifies the large-scale gravitational potential through the same multiplicative factor that governs galactic and cosmological dynamics. For a wave propagating through a region with curvature field $\kappa(r)$, the effective perturbation scales as

$$h_{\rm eff} \propto h_{\rm GR}\, e^{\kappa(r)\, r}\,.$$

Local Mergers: GR Waveforms

Stellar-mass binaries occupy environments where $\kappa r \ll 1$. Expanding the exponential,

$$e^{\kappa r} \simeq 1 + \kappa r,$$

shows that the correction is negligible. The strain, phase evolution and chirp mass reduce to their GR values:

$$g_{\mu\nu}^{(\kappa)} \simeq g_{\mu\nu}^{\rm GR}\,.$$

For systems such as GW170817, the κ-framework reproduces the observed strain amplitude $h \sim 4 \times 10^{-21}$. Thus present-day gravitational-wave detections remain GR-exact.

Primordial Gravitational Waves

In the early universe, densities and velocity gradients were high, and $\kappa(r)$ was correspondingly larger. n this regime $\kappa r \gtrsim 1$, giving

$$h_{\rm prim} \propto h_{\rm GR,prim}\, e^{\kappa_{\rm early}\, r}\,.$$

The model therefore predicts a mild enhancement of the primordial gravitational-wave background and associated CMB B-modes. This provides a direct observational target for future missions sensitive to inflation-scale tensor modes.

Summary

The κ-framework recovers GR waveforms for all known mergers while predicting distinctive signatures in the primordial background. This behaviour aligns with the broader structure-dependent curvature picture established in Sections 8.1–8.6 and offers a falsifiable test of the model.

7.6. Summary of Cosmological Extensions

At recombination the mean baryonic density is high and shear is uniform, so κ contributes negligibly to the background curvature. At late times, as voids dominate and structures develop, κ becomes relevant and produces effects that align with the observed cosmic acceleration, H_0 tension and mild excess lensing. The same parameter that shapes galaxies and rings therefore extends naturally to cosmology without altering early-universe physics.

8. Further Reading

For mathematical foundations and extensions:

Natural Mathematics: Core Axioms and Derived Structure. Pickett, J. (2025). 10.55277/researchhub.13jn6ey6.1

Natural Maths - Mandelbrot Set. Pickett, J. (2025). 10.55277/researchhub.br88fx0d.1

Pickett, J. (2025). Natural Mathematics - Resolution of the Penrose Quantum–Gravity Phase Catastrophe & Connection to the Riemann Spectrum. 10.55277/researchhub.ocyj3cty.1

Pickett, J. (2025). A Prime Curvature Hamiltonian on the Logarithmic Axis with 0.657% Agreement to the Riemann Spectrum. 10.55277/researchhub.m2rtsaxa.1

These explore operator-based geometry and arithmetic ties, providing potential first-principles for $\varkappa$.

Appendix

A.1. Structural Derivation of an Effective Gravitational Constant

The κ-framework modifies the gravitational potential through an environmental curvature response,

$$\Phi_\kappa(r) = -\frac{GM}{r}\, e^{\kappa r},$$

with κ determined by local density and shear. Expanding for $\kappa r \ll 1$,

$$e^{\kappa r} = 1 + \kappa r + \mathcal{O}((\kappa r)^2),$$

gives the effective acceleration:

$$g_\kappa(r) = \frac{GM}{r^2}\, e^{\kappa r} \simeq \frac{GM}{r^2}\left(1 + \kappa r\right).$$

This identifies an effective gravitational constant:

$$G_{\text{eff}}(r) = G\big(1 + \kappa r\big), \qquad (\kappa r \ll 1).$$

Thus, the κ-law produces a direct structural deformation of Newton's constant without introducing new fields or degrees of freedom. The modification is purely geometric and sourced by baryonic structure.

A.1.1. The Structural Origin of G_{eff}

The density–shear definition of κ,

$$\kappa(r) = k_0 \left(\frac{\rho}{\rho_0}\right)^a \left(\frac{r_0}{r}\right)^b + k_v \left(\frac{\partial v/\partial r}{10^{-12}\,\text{s}^{-1}}\right)^3 \left(\frac{\rho}{\rho_0}\right)^{1/2},$$

implies that G_{eff} is not fundamental, but a derived scale determined by the structure of matter surrounding the test mass.

The combination $G(1+\kappa r)$ is therefore the coarse-grained gravitational response of the environment, inherited from the κ-curvature field.

Key structural implications:

1. **In the Solar System,**
   $\kappa r \sim 10^{-12}$ so $G_{\text{eff}} \to G$. This recovers the GR-tested regime precisely.

2. **In galaxies,**
   $\kappa r \sim 10^{-4} - 10^{-3}$ so $G_{\text{eff}} > G$ by an amount sufficient to flatten rotation curves.

3. **In clusters and cosmic basins,**
   $\kappa r \sim 10^{-2}$ so G_{eff} carries the geometric signature of the large-scale cosmic web.

Thus, the κ-law reproduces the observed scale-dependence of gravitational strength using a single geometric mechanism.

A.1.2. Recovering GR in the $\kappa \to 0$ Limit

As structure becomes unresolved (e.g. $r \to \ell_P$ or in idealised homogeneous limits):

$$\lim_{\kappa \to 0} G_{\text{eff}} = G, \qquad \lim_{\kappa \to 0} \Phi_\kappa(r) = -\frac{GM}{r}.$$

The Newtonian and GR weak-field forms are restored exactly and ensures no conflict with:

- Shapiro delay,
- perihelion precession,
- binary pulsars,
- gravitational wave phasing.

The κ-field adds structure-sourced curvature on top of GR's vacuum equations, not in place of them.

A.1.3. Interpretation

The structural reading is:

$$G_{\text{eff}}(r) = G + \Delta G(r), \qquad \Delta G(r) = G\,\kappa r\,.$$

So variation in gravitational strength is not fundamental, but an emergent property of matter distribution, analogous to:

- effective permittivity in dielectrics,
- running couplings in QFT,
- renormalised elastic constants in continuum media.

The gravitational constant measured in a given environment reflects the local curvature weighting applied by κ, not a universal scalar.

A.2. Circular Velocities

For a test mass in a circular orbit of radius r around baryonic mass M, the centripetal acceleration is v^2/r.
Equating this to the κ-modified gravitational acceleration gives

$$\frac{v_\kappa^2}{r} = \frac{GM}{r^2} e^{\kappa r} .$$

Solving for the orbital velocity,

$$v_\kappa(r) = \sqrt{\frac{GM}{r}} e^{\kappa r/2} .$$

The Newtonian prediction from baryons alone is

$$v_N(r) = \sqrt{\frac{GM}{r}} .$$

The ratio between the observed orbital speed

$$v_{\text{obs}}(r)$$

and the baryonic Newtonian prediction defines an empirical κ at that radius:

$$\frac{v_{\text{obs}}}{v_N} = e^{\kappa(r) r/2} .$$

Solving for $\kappa(r)$ yields

$$\kappa(r) = \frac{2}{r}\,\ln\!\left(\frac{v_{\rm obs}(r)}{v_N(r)}\right).$$

This relation is used to infer $\kappa(r)$ directly from rotation-curve data with no dark matter halo. The environmental expression for $\kappa(r)$ in the main text is then fitted to these empirically derived quantities.

A.3. Growth and the Collapse Threshold

The collapse mechanism relies on how κ responds to local structure. The environmental model specifies

$$\kappa(r) = \kappa_0 + k_v \left(\frac{\partial v/\partial r}{10^{-12}\ \mathrm{s}^{-1}}\right)^3 \left(\frac{\rho}{\rho_0}\right)^{1/2}.$$

A.3.1. Density scaling during collapse

For a collapsing region of characteristic radius r:

$$\rho(r) \propto r^{-3}, \qquad \rho^{1/2}(r) \propto r^{-3/2}.$$

A.3.2 Shear scaling during collapse

Velocity gradients grow as the collapse steepens:

$$\frac{\partial v}{\partial r} \;\propto\; \frac{v(r)}{r}.$$

For infall driven by the local potential,

$$v(r) \sim \sqrt{\frac{GM(r)}{r}}.$$

If $M(r)$ changes slowly compared to r, then

$$\frac{\partial v}{\partial r} \sim r^{-3/2}.$$

Thus the shear term scales as

$$\left(\frac{\partial v}{\partial r}\right)^3 \propto r^{-9/2}.$$

A.3.3. Combined scaling

Combining density and shear:

$$\kappa(r) - \kappa_0 \;\propto\; r^{-9/2}\, r^{-3/2} \;=\; r^{-6}.$$

Equivalently,

$$\kappa(r) \;\sim\; r^{-6} \quad \text{as } r \to 0.$$

This expresses the intuition: as a region compresses, κ rises extremely rapidly. A milder scaling can be adopted (for alternative κ-laws), but the qualitative result is unchanged: κ increases sharply as density and shear grow.

A.3.4. Collapse threshold

The weighted gravitational acceleration is

$$g_\kappa(r) = \frac{GM(r)}{r^2}\, e^{\kappa(r) r}.$$

Runaway behaviour begins when the exponential term ceases to be a small correction:

$$\kappa(r)\, r \;\gtrsim\; 1.$$

Substituting the scaling $\kappa \sim r^{-6}$:

$$\kappa(r)\, r \;\sim\; r^{-5}.$$

As r decreases, r^{-5} rises rapidly. There is always a radius r_{crit} where

$$\kappa(r_{\text{crit}})\, r_{\text{crit}} = 1.$$

For $r < r_{\text{crit}}$, the exponential steepening dominates the dynamics:

$$g_\kappa(r) \;\approx\; \frac{GM}{r^2}\exp(r^{-5}),$$

and collapse accelerates beyond any classical counterforce.

A.3.5 Interpretation

The κ-response couples density, shear, and curvature. During compression:

- density increases → $\sqrt{\rho}$ term rises,
- shear sharpens → $(\partial v/\partial r)^3$ term rises,
- κ increases steeply,
- the exponential factor $e^{\kappa r}$ amplifies gravity,
- collapse accelerates until a GR horizon forms.

A.4. Collision-Induced Amplification

We start from the same environmental expression for κ used in the main text:

$$\kappa = \kappa_{\text{base}} + k_v \left(\frac{\nabla v}{10^{-12}\,\text{s}^{-1}}\right)^3 \left(\frac{\rho}{\rho_0}\right)^{1/2}.$$

During a high-velocity cluster collision (relative velocities 3–4×10³ km/s), the effective velocity shear sampled by shocked gas reaches:

$$\nabla v_{\text{rel}} \sim (1\text{–}3)\times 10^{-12}\,\text{s}^{-1}.$$

For the fiducial values $\rho_0 = 1600\,\text{kg m}^{-3}$ and $k_v \approx 5\times 10^{-26}\,\text{m}^{-1}$ this yields:

$$\kappa_{\text{coll}} \approx (1\text{–}5)\times 10^{-23}\,\text{m}^{-1},$$

consistent with the transient increases used in Section 4.3. The lensing deflection becomes:

$$\alpha_{\rm eff}(b) = \alpha_{\rm GR}(b)\, e^{\frac{1}{2}(\kappa_{\rm base}+\kappa_{\rm coll})b}.$$

For a representative impact parameter $b \approx 200\,\mathrm{kpc}$:

$$\kappa_{\rm coll} b \sim 10^{-2}, \qquad e^{\kappa_{\rm coll} b/2} \approx 1.005 - 1.015.$$

Thus the collision temporarily increases the bending angle by 0.5–1.5%, shifting the centre of the lensing map in the same direction as the observed Bullet-Cluster–type offsets. When the shock dissipates, $\nabla v_{\rm rel} \to 0$ and $\kappa_{\rm coll} \to 0$, restoring the original potential.

A.5. Accretion and Early SMBH Growth

Modified Inflow and the κ-Boosted Accretion Rate

The κ-framework modifies the gravitational potential through

$$\Phi_\kappa(r) = -\frac{GM}{r}\, e^{\kappa r},$$

leading to an effective acceleration

$$g_\kappa(r) = \frac{GM}{r^2}\, e^{\kappa r}.$$

In spherical inflow, the Bondi accretion rate is

$$\dot{M}_{\rm Bondi} = 4\pi\lambda\, \frac{(GM)^2 \rho_\infty}{c_s^3},$$

where c_s is the sound speed and ρ_∞ is the ambient density.

In the κ-framework, the increase in gravitational acceleration effectively rescales the gravitational coupling by

$$G \longrightarrow G_{\rm eff}(r) = G\, e^{\kappa r}.$$

Because $\dot{M} \propto G^2$, the κ-modified accretion rate becomes

$$\dot{M}_\kappa \;=\; \dot{M}_{\rm Bondi}\, e^{2\kappa r}\,.$$

For steady inflow near the Schwarzschild radius, take $r \approx r_s \equiv 2GM/c^2$. Then

$$\dot{M}_\kappa = \dot{M}_{\rm Bondi}\, \exp\!\left(\frac{4GM\kappa}{c^2}\right)$$

Even modest values of $\kappa r_s \sim 0.1{-}0.3$ give order-of-magnitude boosts:

$$e^{4\kappa r_s} \sim 3{-}30.$$

This provides a natural, geometry-driven enhancement to growth rates without invoking super-Eddington physics or departures from radiative efficiency.

A.5.1. Departure from the Eddington Limit

The Eddington-limited growth equation

$$\dot{M}_{\rm Edd} = \frac{M}{t_{\rm Sal}}, \qquad t_{\rm Sal} \simeq 4.5\times10^7\ {\rm yr},$$

is replaced by

$$\dot{M} = \frac{M}{t_{\rm Sal}}\, e^{2\kappa r_s}\,.$$

Thus

$$M(t) = M_0\, \exp\left[\frac{t}{t_{\rm Sal}}\, e^{2\kappa r_s}\right] .\,].$$

With a κ-boost of only $e^{2\kappa r_s} \sim 5$, the effective growth timescale becomes

$$t_{\rm eff} = \frac{t_{\rm Sal}}{5} \simeq 9\,{\rm Myr},$$

sufficient to grow $10^3-10^4\,M_\odot$ seeds to $10^8-10^9\,M_\odot$ in under a giga-year — matching JWST observations.

A.6. Primordial Collapse Scale and the Horizon-Mass Relation

κ-Triggered Collapse in the Early Universe

At early times the density and shear fields are large, yielding a background κ close to the environmental upper limit. The collapse criterion is

$$\kappa r \gtrsim 1.$$

For a collapsing over-density of physical radius $r(t)$, the condition becomes

$$\kappa(t)\, r(t) \approx 1 \quad \Rightarrow \quad r(t) \approx \kappa(t)^{-1}\,.$$

The mass contained inside that radius is

$$M(t) = \frac{4\pi}{3}\,\rho(t)\, r(t)^3 = \frac{4\pi}{3}\,\rho(t)\,\kappa(t)^{-3}\,.$$

During radiation domination, the horizon mass is

$$M_H(t) \approx \frac{c^3 t}{G}\,.$$

To be consistent with standard PBH formation should show that:

$$M(t) \propto M_H(t)\,.$$

A.6.1. Demonstrating Consistency with the Horizon-Mass Scaling

Take $\kappa(t)$ scaling from the main model:

$$\kappa(t) \propto \rho(t)^{1/2}\,.$$

During radiation domination:

$$\rho(t) \propto t^{-2} \quad \Longrightarrow \quad \kappa(t) \propto t^{-1}\,.$$

Thus

$$r(t) = \kappa^{-1}(t) \propto t,$$

and therefore

$$M(t) \propto \rho(t)\, r(t)^3 \propto t^{-2}\, t^3 \propto t\,.$$

But $M_H(t) \propto t$. Hence

$$M_{\mathrm{PBH}}(t) \;\propto\; M_H(t)$$

This is the standard primordial black hole mass relation — and it arises directly from the κ -framework without tuning.

A.6.2. Interpretation

Because $r \sim \kappa^{-1}$ and $\kappa \propto \rho^{1/2}$, the physical scale of instability always tracks the Hubble length during radiation domination. Consequently:

- κ-triggered collapse naturally occurs at the horizon scale.
- The mass of the resulting black hole matches the expected PBH spectrum.
- No exotic physics or additional fields are introduced.
- The same collapse law that operates in galactic nuclei operates in the early universe.

A.7. Gravitational Lensing

In standard General Relativity, the deflection angle for a photon passing mass M with impact parameter

$$\alpha_{\mathrm{GR}}(b) = \frac{4GM}{c^2 b}\,.$$

The κ-dependent potential introduces an exponential correction to the same expression. In the weak-field limit the effective deflection angle becomes

$$\alpha_{\rm eff}(b) = \alpha_{\rm GR}(b)\, e^{\kappa b/2} = \left(\frac{4GM}{c^2 b}\right) e^{\kappa b/2}\,.$$

For $\kappa b \ll 1$, the exponential expands to

$$\alpha_{\rm eff}(b) \approx \alpha_{\rm GR}(b)\left(1+\tfrac{1}{2}\kappa b\right),$$

showing that κ introduces a scale-dependent enhancement of the deflection without altering the underlying baryonic mass distribution.

A.8. Environmental Density and Shear

The geometric origin of κ implies that it depends on local structure. An observationally motivated expression used in the main text is

$$\kappa(r) = \kappa_0 \;+\; k_v \left(\frac{\partial v/\partial r}{10^{-12}\,\mathrm{s}^{-1}}\right)^3 \left(\frac{\rho}{\rho_0}\right)^{1/2}.$$

Parameters and quantities:

- κ_0 : background curvature level
- k_v : shear-response coefficient
- $\partial v/\partial r$: local velocity gradient (shear)
- ρ/ρ_0 : density relative to fiducial scale

The cubic response to shear highlights regions of strong differential rotation (e.g., spiral arms, shocked gas in mergers), while the square-root density term captures curvature enhancement in compressed environments relative to voids.

When this $\kappa(r)$ expression is placed into the velocity and lensing formulae, the resulting predictions match rotation curves and lensing profiles across many systems using baryonic matter alone.

A.9. Effective Cosmic Acceleration

At cosmic scales, κ is dominated by the average structure of the cosmic web: voids, walls, filaments, and superclusters. In this regime, κ varies slowly and is well approximated by a background value κ_0.

In a homogeneous background, the κ-modified gravitational response produces an additive term in the acceleration equation:

$$\frac{\ddot{a}}{a} = -\frac{4\pi G}{3}\rho_{\text{eff}} + \mathcal{A}(\kappa_0),$$

where $\mathcal{A}(\kappa_0)$ is an effective acceleration generated by the large-scale κ-field.

For background values of κ_0 consistent with structure formation and supercluster flows, $\mathcal{A}(\kappa_0)$ attains the same magnitude as the late-time cosmic acceleration usually attributed to Λ with the acceleration emerging from structure-dependent curvature.

The precise mapping between $\mathcal{A}(\kappa_0)$ and a Λ-like parameter depends on the averaging prescription, but the qualitative behaviour follows directly from the same κ-dependent potential used at galactic and cluster scales.

A.10. Induced Hubble Shift

In the κ-framework, local departures from the homogeneous FRW background arise from density- and shear-dependent curvature. A galaxy embedded within a coherent over-density of characteristic size r_{loc} experiences a slightly modified recession rate relative to the global value $H_0^{(\text{CMB})}$.

For slowly varying κ, the first-order correction to the local expansion rate is

$$H_0^{(\kappa)} \simeq H_0^{(\text{CMB})}\left(1 + \beta\,\kappa\, r_{\text{loc}}\right),$$

where κ is the large-scale background value, r_{loc} is the coherence scale of the local flow ($\approx$ 50–150 Mpc), and β encodes how efficiently κ-dependent curvature gradients couple to the inferred expansion rate (typically 1–2 from simulations of basin flows).

A.10.1. Numerical Input

Representative large-scale values inferred from supercluster-scale flows:

$$\kappa_0 \;=\; 2.6 \times 10^{-26}\,\mathrm{m}^{-1} \;=\; 8.0 \times 10^{-4}\,\mathrm{Mpc}^{-1}\,.$$

Local coherence scale:

$$r_{\mathrm{loc}} \;\approx\; 100\,\mathrm{Mpc}\,.$$

Dimensionless combination:

$$\kappa_0\, r_{\mathrm{loc}} \;=\; (8.0 \times 10^{-4})(100) \;=\; 0.080.$$

Coupling coefficient (from κ-driven flow fields):

$$\beta \;\approx\; 1.1.$$

A.10.2. Result

$$H_0^{(\kappa)} \;\simeq\; H_0^{(\mathrm{CMB})}\left(1 + \beta\,\kappa_0 r_{\mathrm{loc}}\right)$$

$$=\; H_0^{(\mathrm{CMB})}\left(1 + 1.1 \times 0.080\right)$$

$$=\; H_0^{(\mathrm{CMB})}\,(1 + 0.088)$$

$$\Rightarrow \qquad H_0^{(\kappa)} \;\approx\; 1.088\,H_0^{(\mathrm{CMB})}\,.$$

Taking the Planck value $H_0^{(\mathrm{CMB})} = 67\,\mathrm{km\,s^{-1}\,Mpc^{-1}}$:

$$H_0^{(\kappa)} \;\approx\; 67 \times 1.088 \;\approx\; 72.9\,\mathrm{km\,s^{-1}\,Mpc^{-1}}\,.$$

A.10.3. Interpretation

A background curvature coefficient of order

$$\kappa_0 \sim 10^{-26}\,\mathrm{m}^{-1}$$

naturally generates an 8–9% enhancement of the locally inferred expansion rate across coherence scales of ~100 Mpc. The scale of the shift matches the observed Planck–SH0ES tension without introducing additional components or relativistic species.

A.11. Mass-Energy Equivalence Under $\kappa(r)$

In the κ-modified weak-field limit, the gravitational potential is

$$\Phi_\kappa(r) = -\frac{GM}{r}\, e^{\kappa r}\,.$$

Differentiating gives the radial acceleration:

$$g_\kappa(r) = \frac{GM}{r^2}\, e^{\kappa r}\,.$$

It is often convenient to express the exponential factor as a scale-dependent gravitational weight:

$$g_\kappa(r) = \frac{GM}{r^2}\left(\frac{m_{\text{grav}}(r)}{m}\right), \qquad m_{\text{grav}}(r) = m\, e^{\kappa r}\,.$$

This quantity $m_{\text{grav}}(r)$ is not a change to the particle's intrinsic mass. It captures how the curvature field weights the gravitational interaction at scale r. Inertial mass remains constant, and the local relation $E = mc^2$

The curvature-weighted gravitational energy takes the same form,

$$E_\kappa(r) = mc^2\, e^{\kappa r}\,.$$

At small radii, where $\kappa r \ll 1$, the exponential term disappears and the standard expression is recovered:

$$\lim_{r\to 0} E_\kappa(r) = mc^2\,.$$

This yields a clear distinction: inertial mass and special-relativistic energy remain fixed, while the gravitational influence of that energy is modulated by the local field. The κ

-framework therefore introduces a scale-dependent gravitational response without altering local relativistic physics.

A.12. The Quantum Limit

To examine the behaviour of the κ-weighted potential near the quantum domain, begin with

$$\Phi_\kappa(r) = -\frac{GM}{r}\, e^{\kappa(r)\, r}\,.$$

Here $\kappa(r)$ is an effective structural parameter built from coarse-grained density, gradients, and shear. At scales where structure cannot be resolved (approaching the Planck length) κ must approach zero.

A.12.1. Small-r expansion

For any finite $\kappa(r)$, the exponential has a Taylor expansion around

$$e^{\kappa(r)\, r} = 1 + \kappa(r)\, r + \tfrac{1}{2}\kappa(r)^2 r^2 + \mathcal{O}(r^3)\,.$$

Substituting:

$$\Phi_\kappa(r) = -\frac{GM}{r}\left[1 + \kappa(r)\, r + \tfrac{1}{2}\kappa(r)^2 r^2 + \mathcal{O}(r^3)\right].$$

Expanding term-by-term:

$$\Phi_\kappa(r) = -\frac{GM}{r} \;-\; GM\,\kappa(r) \;-\; \tfrac{1}{2}GM\,\kappa(r)^2 r \;+\; \mathcal{O}(r^2)\,.$$

The $1/r$ behaviour is unchanged. All -dependent terms remain finite or vanish as $r \to 0$. Thus the short-distance structure of the potential is exactly the Newtonian (and GR) form.

A.12.2. κ sourced by macroscopic structure

In the κ-r framework, $\kappa(r)$ is defined through measurable, resolvable structure:

$$\kappa(r) = \kappa_0 + k_v \left(\frac{\partial v/\partial r}{10^{-12}\,\mathrm{s}^{-1}} \right)^3 \left(\frac{\rho}{\rho_0} \right)^{1/2}.$$

As $r \to \ell_P$, matter distribution is effectively homogeneous and all resolvable gradients vanish because the resolution scale falls below any physical inhomogeneity. Consequently,

$$\lim_{r\to\ell_P} \kappa(r) = 0, \qquad \lim_{r\to\ell_P} \Phi_\kappa(r) = -\frac{GM}{r}.$$

A.12.3. κ weighted mass–energy

The κ-weighted inertial energy is

$$E_\kappa(r) = mc^2 e^{\kappa(r)r}.$$

Expanding:

$$E_\kappa(r) = mc^2\left[1 + \kappa(r)r + \frac{1}{2}\kappa(r)^2 r^2 + \mathcal{O}(r^3)\right].$$

Thus,

$$\lim_{r\to\ell_P} E_\kappa(r) = mc^2.$$

Inertial mass remains unchanged; κ supplies only a gravitational weighting that disappears in the quantum limit.

A.12.4. Interpretation

κ acts as a structural modifier. It vanishes when structure cannot be resolved (Planck scale) and grows as soon as macroscopic density contrasts, gradients, and shear emerge. The κ -framework therefore transitions cleanly:

- **Quantum regime:** $\kappa \to 0$, standard Newtonian/GR behaviour recovered.
- **Macroscopic regime:** $\kappa \neq 0$, curvature responds to structure.

This establishes a scale-dependent but coherent connection between microscopic gravity and κ-modified macroscopic law.

References

Clemence, G. M. (1947). AJ, 53, 169

Lin, C. C., & Shu, F. H. (1964). ApJ, 140, 646

Boylan-Kolchin, M. (2023). Nature Astronomy, 7, 731

Carnall, A. C. et al. (2024). MNRAS (submitted)

Carr, B. et al. (2020). Phys. Rep., 905, 1

Rubin, V. et al. (1970). ApJ, 159, 379

Clowe, D. et al. (2006). ApJ, 648, L109

Planck Collaboration (2020). A&A, 641, A6

DESI Collaboration (2024). ApJ (submitted)

Milgrom, M. (1983). ApJ, 270, 371

Sanders, R., & McGaugh, S. (2002). ARAA, 40, 263

Famaey, B., & McGaugh, S. (2012). Living Rev. Rel., 15, 10

Bekenstein, J. (2004). Phys. Rev. D, 70, 083509

Verlinde, E. (2017). SciPost Phys., 2, 016

Cognola, G. et al. (2008). Phys. Rev. D, 77, 046009